Electronic Supplementary Material (ESI) for CrystEngComm.
This journal is © The Royal Society of Chemistry 2021

**Supporting Information**

# Preyssler-type Polyoxometalate-based Crystalline Materials for Electrochemical Detection of $H_2O_2$

Haotian Zhu‡[a], Wensi Tang‡[a], Yuanyuan Ma*[a,b], Yonghui Wang[a], Huaqiao Tan[a], Yangguang Li*[a]

*a. Polyoxometalate Science of Ministry of Key Laboratory of Education, Faculty of Chemistry, Northeast Normal University, Ren Min Street No. 5268, Changchun, Jilin, 130024, P. R. China, E-mail: liyg658@nenu.edu.cn*
*b. College of Chemistry and Material Science, Hebei Normal University, Shijiazhuang, Hebei 050024, P. R. China, E-mail: mayy334@hebtu.edu.cn*

**Contents**

==========

**1. Crystal structure figures ..... Page 1**

**2. Physical characterizations ..... Page 5**

**3. Electrocatalytic properties ..... Page 9**

**4. Selected bond lengths and angles of compounds ..... Page 13**

==========

## 1. Supplementary figures

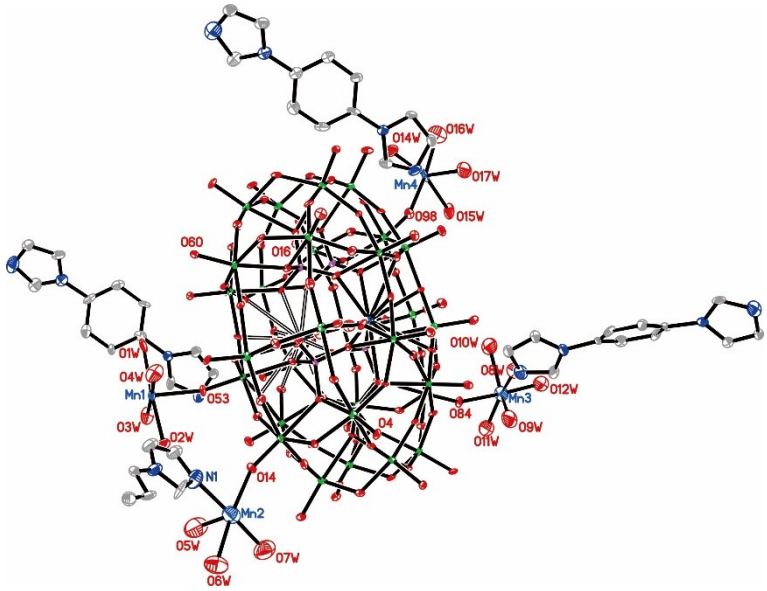


**Figure S1** ORTEP view of the asymmetric unit of compound **1** with atom labeling (30% probability displacement ellipsoids; Hydrogen atoms and lattice water molecules have been omitted for clarity)

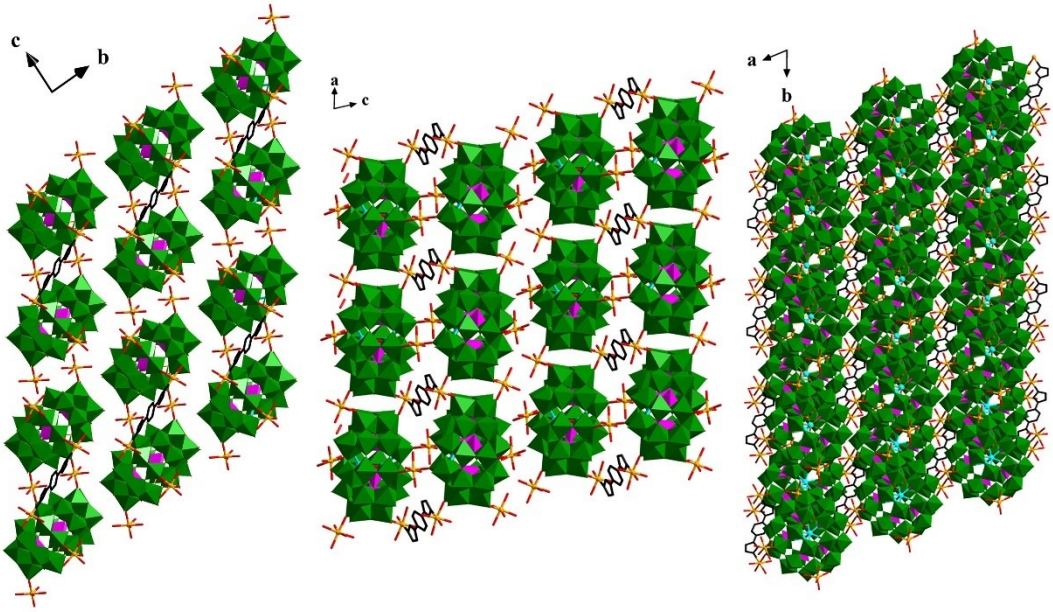


**Figure S2** Polyhedral and ball-and-stick representation of a 3-D structure of compound **1** packing arrangement along a (a), b (b), and c (c) axes, respectively (hydrogen atoms and lattice water molecules have been omitted for clarity).

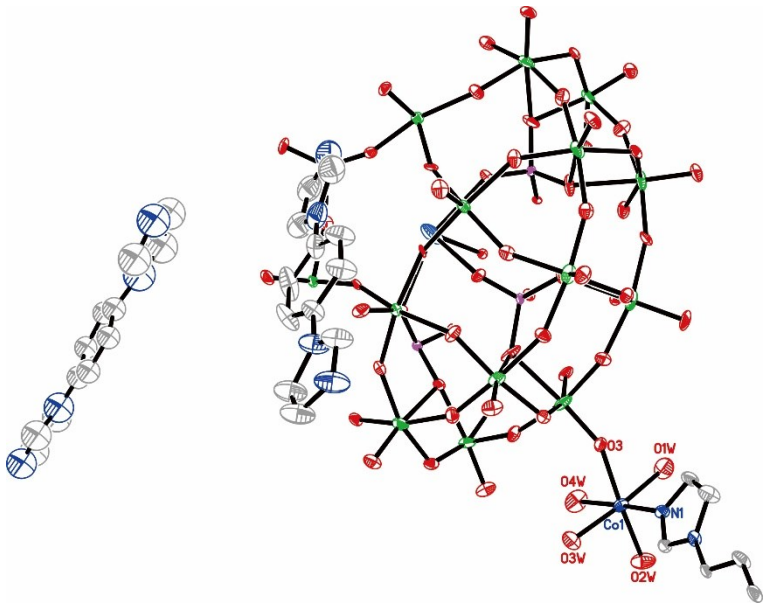


**Figure S3** ORTEP view of the asymmetric unit of compound **2** with atom labeling (30% probability displacement ellipsoids; Hydrogen atoms and lattice water molecules have been omitted for clarity).

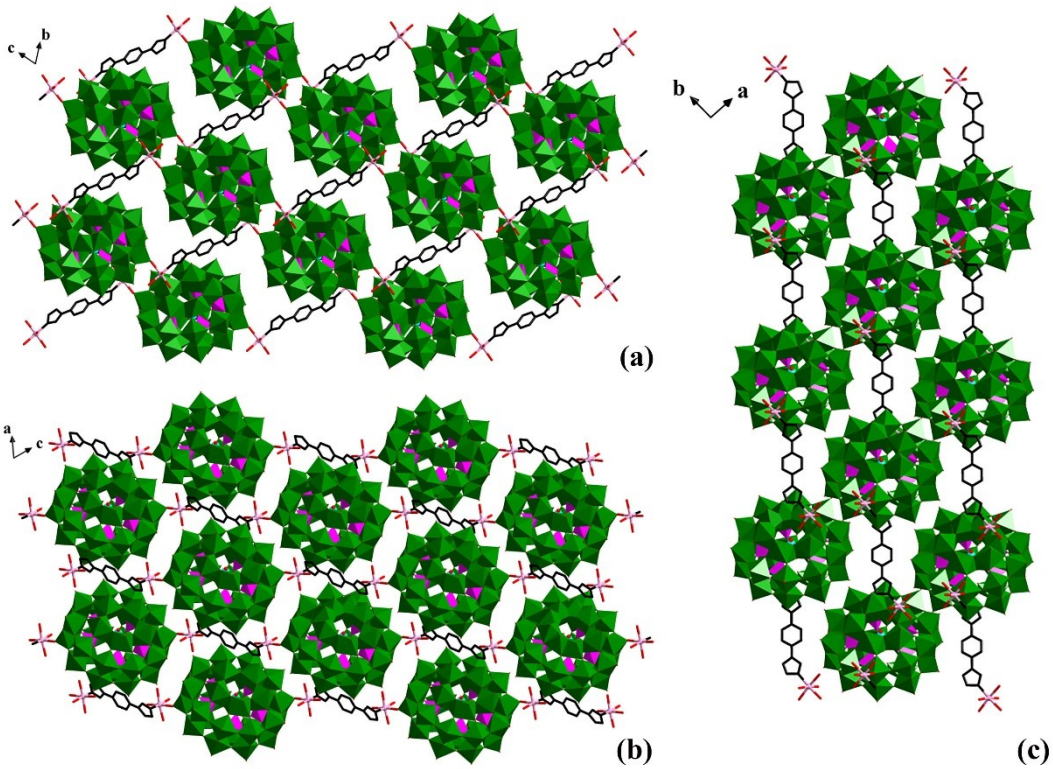


**Figure S4** Polyhedral and ball-and-stick representation of a 3-D structure of compound **2** packing arrangement along a (a), b (b), and c (c) axes, respectively (hydrogen atoms and lattice water molecules have been omitted for clarity)

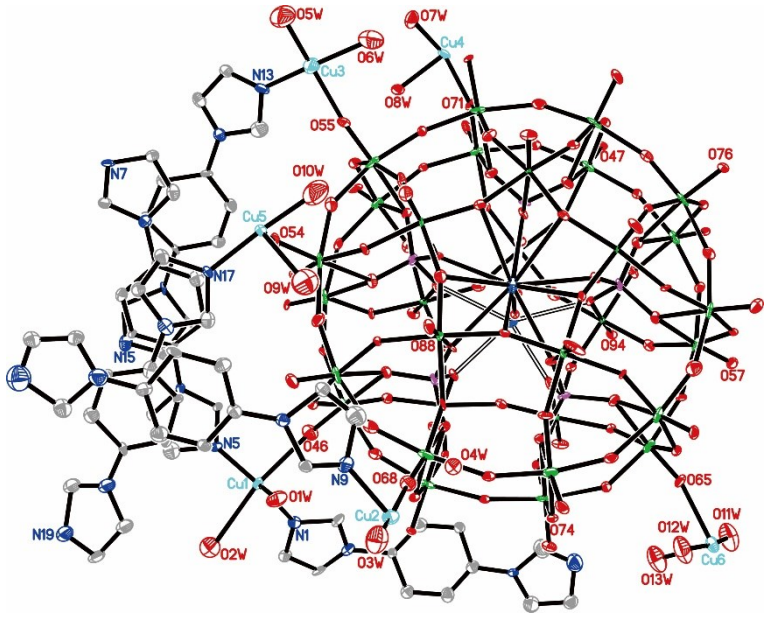


**Figure S5** ORTEP view of the asymmetric unit of compound **3** with atom labeling (30% probability displacement ellipsoids; Hydrogen atoms and lattice water molecules have been omitted for clarity)

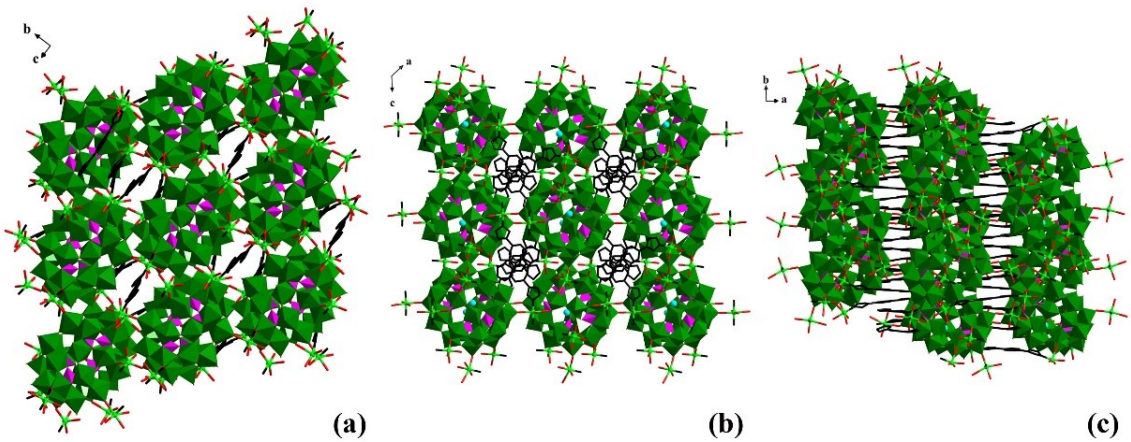


**Figure S6** Polyhedral and ball-and-stick representation of a 3-D structure of **compound 3** packing arrangement along a (a), b (b), and c (c) axes, respectively (hydrogen atoms and lattice water molecules have been omitted for clarity)

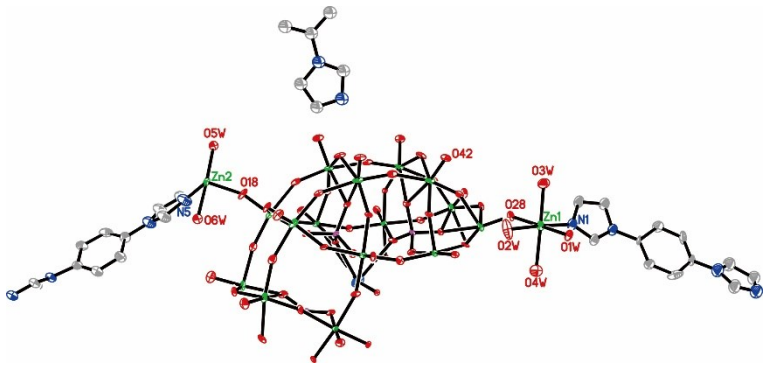


**Figure S7** ORTEP view of the asymmetric unit of compound **4** with atom labeling (30% probability displacement ellipsoids; Hydrogen atoms and lattice water molecules have been omitted for clarity)

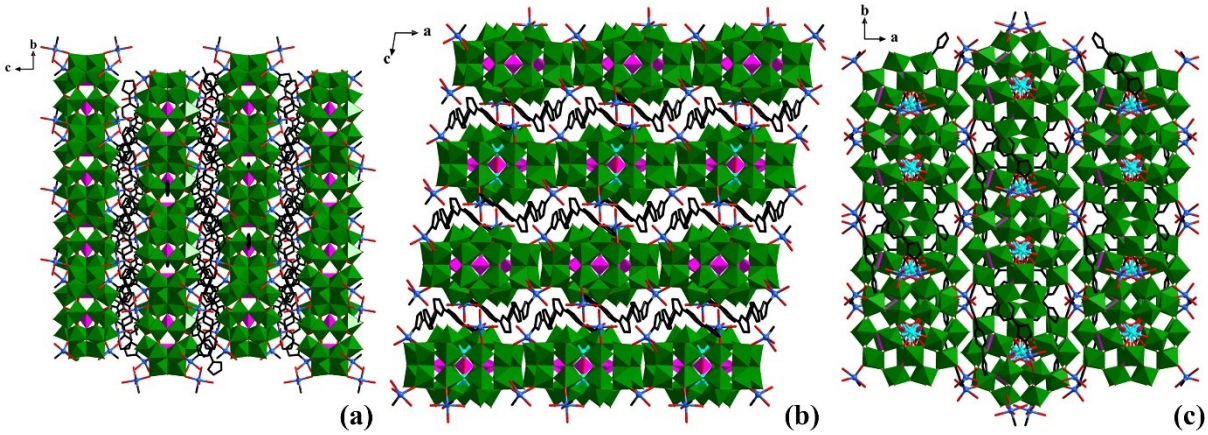


**Figure S8** Polyhedral and ball-and-stick representation of a 3-D structure of **compound 4** packing arrangement along a (a), b (b), and c (c) axes, respectively (hydrogen atoms and lattice water molecules have been omitted for clarity)

## 2. Physical characterizations

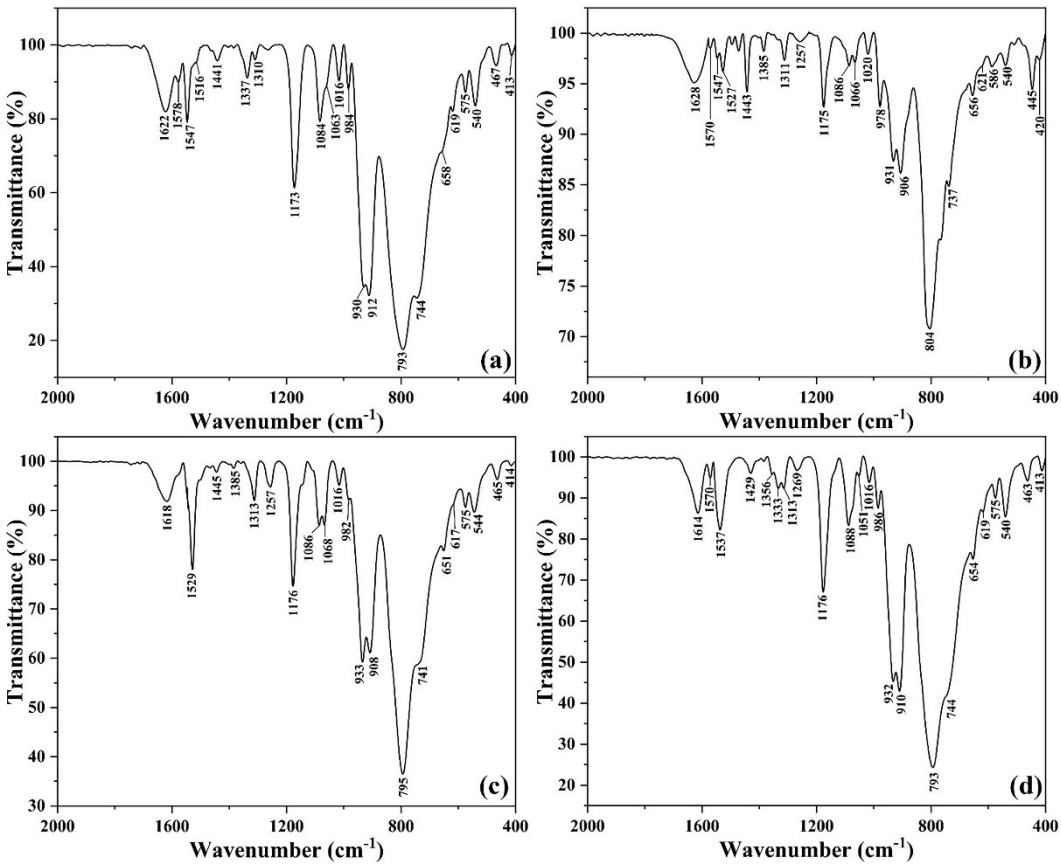


**Figure S9** (a-d) IR spectra of compounds **1-4** from 4000 to 400 $cm^{-1}$.

As shown on Figure S9†, the bands at 3448–3510 $cm^{-1}$ are attributed to *v*(O–H), and the bands at 2853–3136 $cm^{-1}$ are belonged to *v*(N–H) and *v*(C–H) of bimb molecules. The bands at 1051–1176 $cm^{-1}$ are attributed to *v*(P–O). The split bands at 906–933 $cm^{-1}$ are attributed to *v*(W=$O_{terminal}$), while the strong 737–804 $cm^{-1}$ are attributed to *v*(W/TM–$O_{b,c}$–W/TM, TM = Mn, Co, Cu, Zn), respectively ($O_{b,c}$ are bridging O atoms). The bands at 1257–1628 $cm^{-1}$ are associated with bimb ligands.

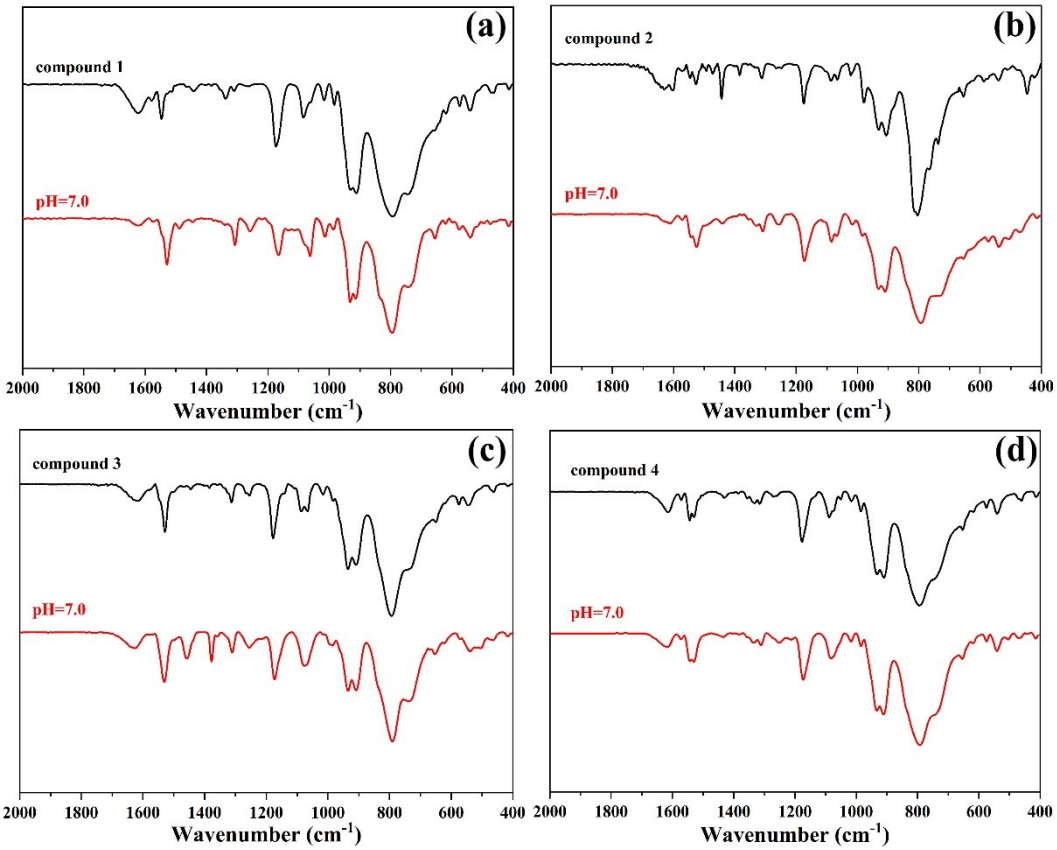


**Figure S10** (a-d) IR spectra from 2000 to 400 $cm^{-1}$ of compounds **1-4** before and after soaking in pH 7.0 PBS solution for 24 h, respectively.

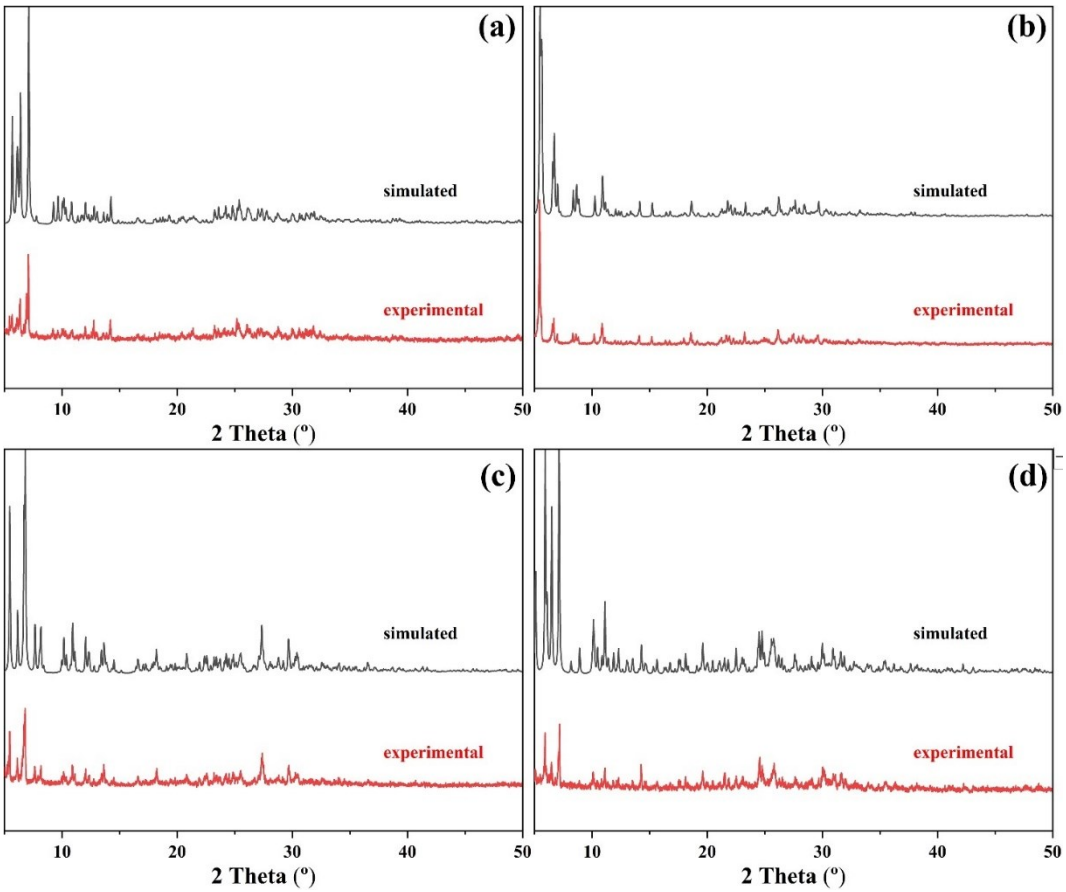


**Figure S11** (a-d) The simulated and experimental XRD patterns of compound **1-4.**

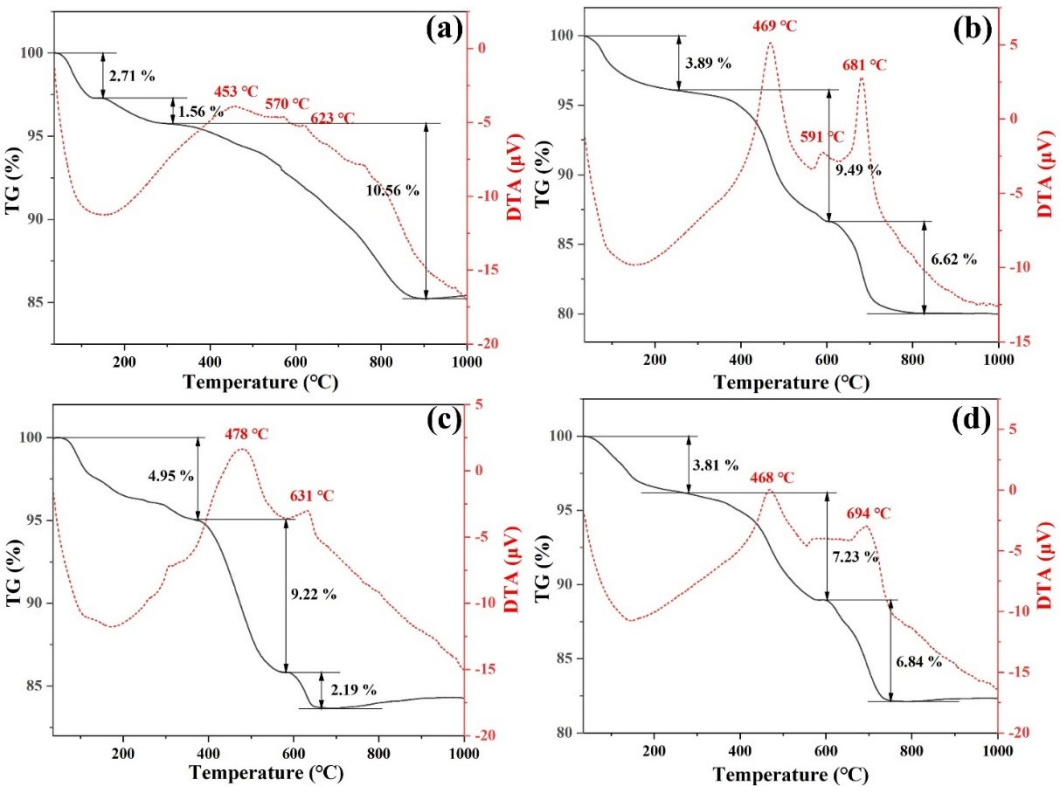


**Figure S12** (a-d) TG-DTA curve of compound **1-4**

As seen from Figure S12a†, the TG curve of compound **1** shows two step weight losses from 33 to 1000 °C. The first weight loss of 2.71 % from 33 to 150 °C is accordance with the theoretical value (3.09 %), which is attributed to lose all lattice water molecules. The second weight loss of 1.56 % from 150 to 313 °C is attributed to combustion of a $H_2$bimb molecule with the theoretical value (1.18 %). The third continuous weight loss of 10.56 % in the range of 313−905 °C is higher than theoretical loss (9.70 %) attributed to combustion of other $H_2$bimb molecules. The three exothermal peaks observed at 453, 570 and 623 °C in DTA curve are assigned to the combustion of $H_2$bimb molecules. This result indicates that the structure of compound **1** has a good thermal stability before 313 °C.

The TG curve of compound **2** shows three steps from 33 to 1000 °C (Figure S12b†). The first weight loss of 3.89 % from 33 to 230 °C is accordance with the theoretical value (3.91 %), which is attributed to lose all water molecules. The second weight loss of 9.49 % in the range of 230−605 °C corresponded to the theoretical loss (9.71 %) of all $H_2$bimb molecules. In DTA curve, there are two obvious exothermal peaks observed at 469 and 591 °C. They are assigned to the combustion of $H_2$bimb molecules. And the third weight loss of 6.62 % in the range of 605−835 °C may be due to part decomposition of POM skeleton. This corresponds to the obvious exothermal peak observed at 681 °C in DTA curve. This result indicates that the structure of compound **2** has a good thermal stability before 230 °C.

The TG curve of compound **3** shows three steps from 33 to 1000 °C (Figure S12c†). The first weight loss of 4.95 % from 33 to 363 °C is accordance with the theoretical value (4.67 %), which is attributed to lose all water molecules. The second and third weight loss of 9.22 % and 2.19 % in the range of 363−582 °C and 582−685 °C together corresponded to the theoretical loss (11.46 %) of all $H_2$bimb molecules. In DTA curve, there are two obvious exothermal peaks observed at 478 and 631 °C, which assigned to the combustion of $H_2$bimb molecules. This result indicates that the structure of compound **3** has a good thermal stability before 363 °C.

The TG curve of compound **4** shows three steps from 33 to 1000 °C (Figure S12d†). The first weight loss of 3.81 % from 33 to 270 °C is accordance with the theoretical value (3.78 %), which is attributed to lose all water molecules. The second and third weight loss of 7.23 % and 6.84 % in the range of 270−588 °C and 588−785 °C together higher than the theoretical loss (11.70 %) of all $H_2$bimb molecules. This may be due to part decomposition of POM skeleton, which corresponds to the obvious exothermal peak observed at 694 °C in DTA curve. And there is another peak observed at 468 °C, which assigned to the combustion of $H_2$bimb molecules. This result indicates that the structure of compound **4** has a good thermal stability before 270 °C.

## 3. Electrocatalytic properties

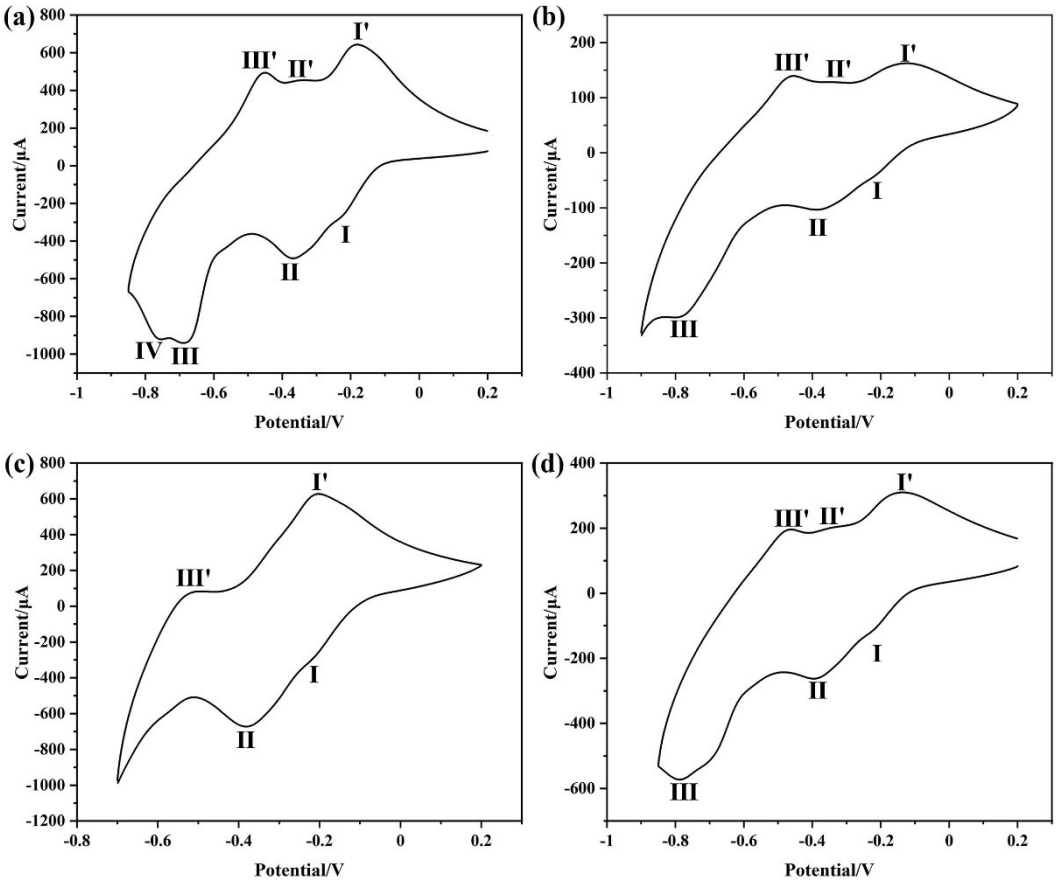


**Figure S13** (a-d) The CV curves of compounds **1-4** in 0.5M $H_2SO_4$.

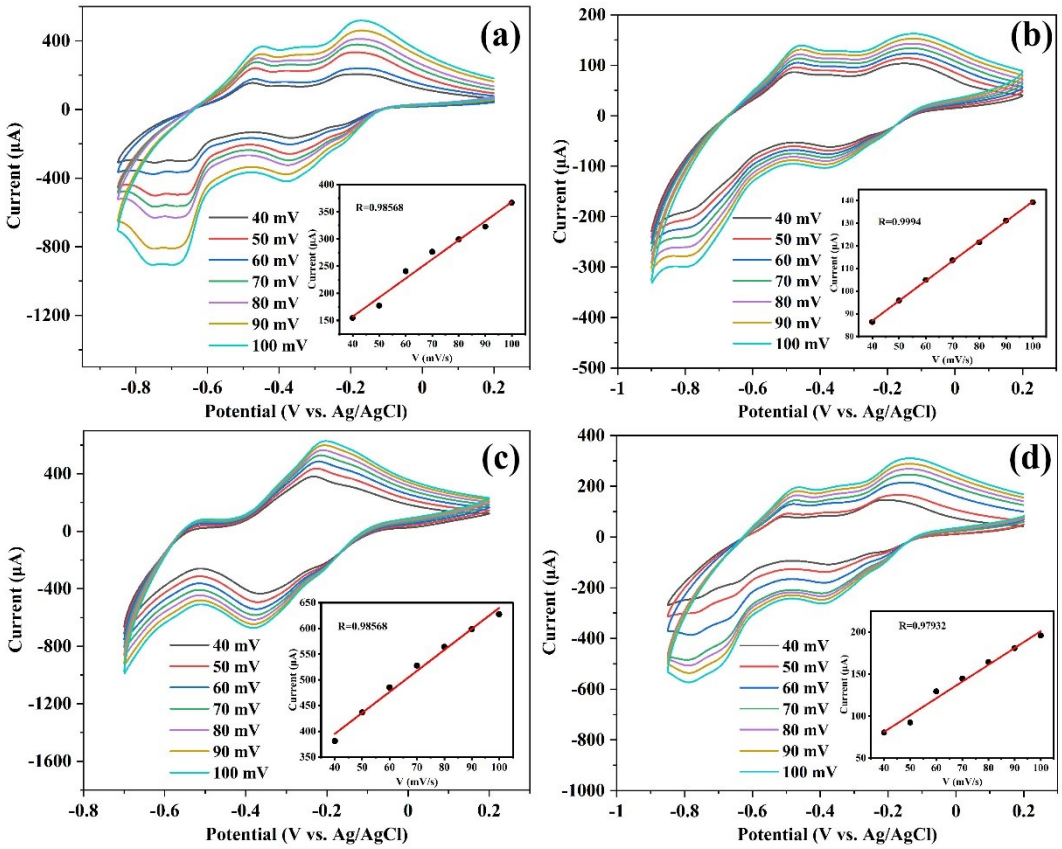


**Figure S14** (a-d) CV as a function of the scan rate for compounds **1-4** in 0.5 M $H_2SO_4$. Inset: variation of the oxidation peak current intensity as a function of the scan rate.

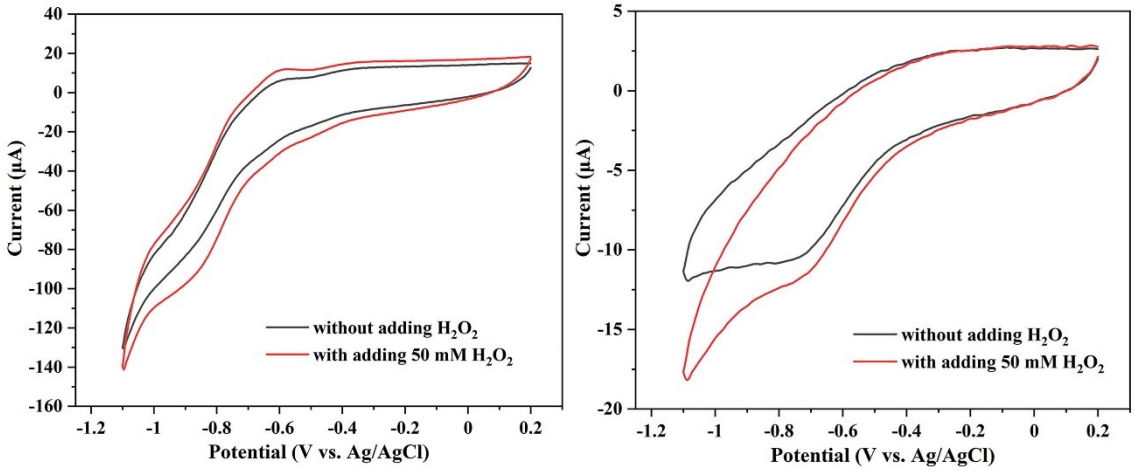


**Figure S15** The CV curves of (a) Co-$P_5W_{30}$; (b) bimb-$P_5W_{30}$ in 0.1 M PBS electrolyte with or without adding 5 mM $H_2O_2$.

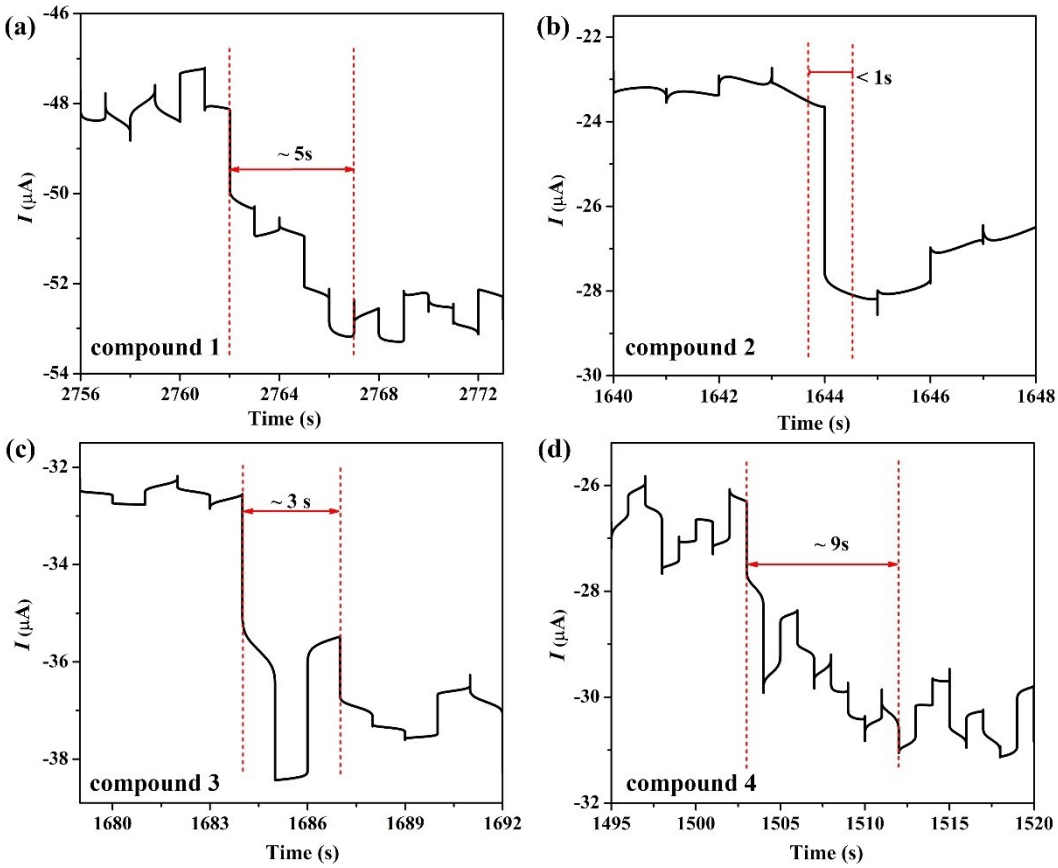


**Figure S16** (a-d) The electrochemical response time of compounds **1-4** toward $H_2O_2$ detection.

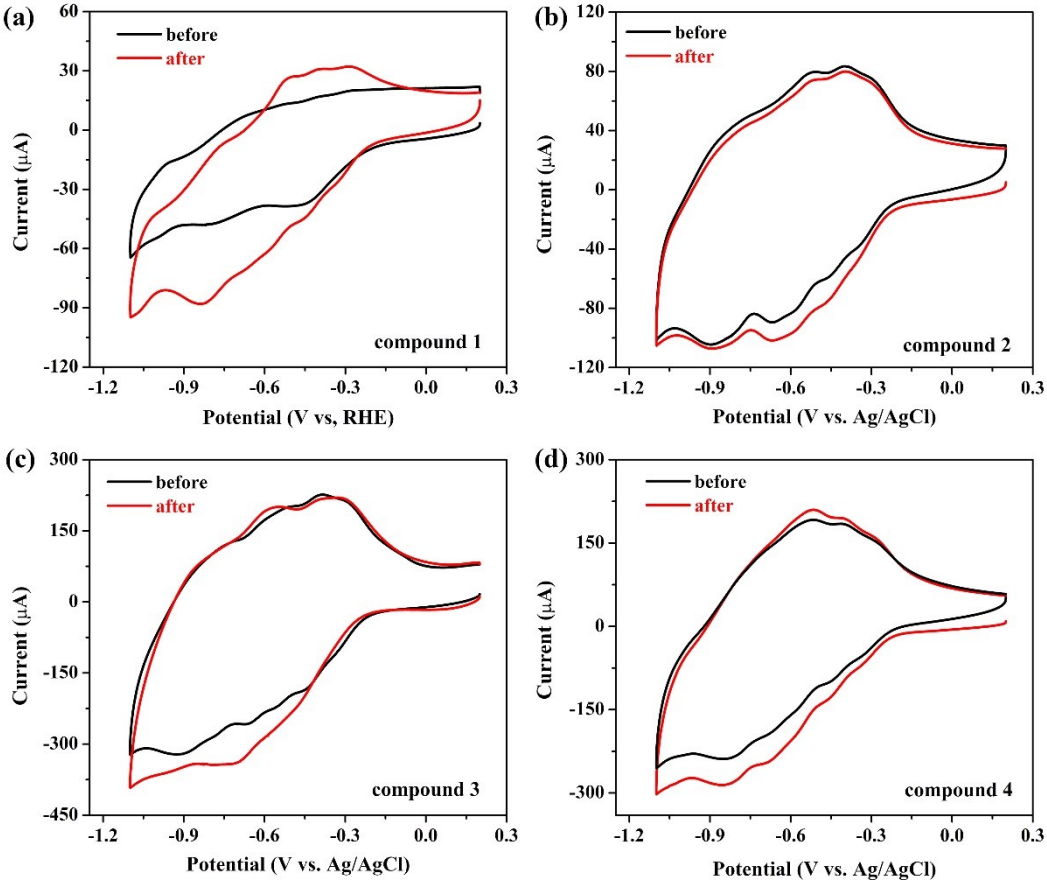


**Figure S17** (a-d) The CV curves of compounds **1-4** before and after the electrochemical detection of $H_2O_2$.

## 4. Selected bond lengths and angles of compounds

**Table S1** Selected bond lengths (Å) and angles (°) for compound **1**

| Bond | Length(Å) | Bond | Length(Å) | Bond | Length(Å) |
|---|---|---|---|---|---|
| Mn1–O60#1 | 2.107(12) | Mn2–O14 | 2.186(13) | Mn3–O11W | 2.32(4) |
| Mn1–O53 | 2.111(12) | Mn2–O5W | 2.19(2) | Mn3–O10W | 2.36(4) |
| Mn1–O2W | 2.167(15) | Mn2–O16#2 | 2.201(13) | Mn4–O16W | 2.17(5) |
| Mn1–O3W | 2.170(15) | Mn2–O6W | 2.29(2) | Mn4–O98 | 2.182(17) |
| Mn1–O4W | 2.236(16) | Mn3–O9W | 1.98(3) | Mn4–O4#3 | 2.205(16) |
| Mn1–O1W | 2.244(16) | Mn3–O8W | 2.06(4) | Mn4–O17W | 2.212(10) |
| Mn2–O7W | 2.16(3) | Mn3–O84 | 2.08(2) | Mn4–O14W | 2.23(4) |
| Mn2–N1 | 2.19(2) | Mn3–O12W | 2.13(4) | Mn4–O15W | 2.25(4) |
| **Bond** | **Angle(°)** | **Bond** | **Angle(°)** | **Bond** | **Angle(°)** |
| O60#1–Mn1–O53 | 175.9(5) | O7W–Mn2–O5W | 84.0(10) | O16W–Mn4–O98 | 170.8(16) |
| O60#1–Mn1–O2W | 92.3(5) | O16#2–Mn2–O6W | 82.7(7) | O16W–Mn4–O4#3 | 95.7(12) |
| O60#1–Mn1–O3W | 93.3(6) | O9W–Mn3–O8W | 63.7(13) | O16W–Mn4–O17W | 88.2(17) |
| O4W–Mn1–O1W | 88.6(7) | O9W–Mn3–O84 | 74.9(10) | O14W–Mn4–O15W | 162.5(14) |
| O7W–Mn2–N1 | 177.0(10) | O9W–Mn3–O12W | 111.4(15) | | |
| O7W–Mn2–O14 | 97.2(9) | O11W–Mn3–O10W | 109.1(14) | | |

Symmetry transformations used to generate equivalent atoms: #1 -x,-y+1,-z+2; #2 x+1,y,z; #3 x-1,y,z

**Table S2** Hydrogen bonds for compound **1**

| D–H···A | d(D–H) | d(H···A) | d(D···A) | <(DHA) |
|---|---|---|---|---|
| N3–H3B···O106 | 0.86 | 1.94 | 2.72(2) | 150.0 |
| N5–H5B···O7W#6 | 0.86 | 2.42 | 3.13(4) | 139.2 |
| N7–H7A···O14W#7 | 0.86 | 2.03 | 2.89(4) | 173.5 |
| N11–H11A···O102#8 | 0.86 | 2.62 | 3.25(2) | 130.3 |
| N13–H13B···O67 | 0.86 | 2.12 | 2.88(2) | 147.2 |

Symmetry transformations used to generate equivalent atoms: #6 x-1,y+1,z; #7 -x-1,-y+1,-z+2; #8 x+1,y,z-1

**Table S3** Selected bond lengths (Å) and angles (°) for compound **2**

| Bond | Length(Å) | Bond | Length(Å) | Bond | Length(Å) |
|---|---|---|---|---|---|
| Co1–N1 | 2.069(12) | Co1–O3W | 2.087(13) | Co1–O1W | 2.098(13) |
| Co1–O3 | 2.081(10) | Co1–O2W | 2.090(12) | Co1–O4W | 2.123(13) |
| **Bond** | **Angle(°)** | **Bond** | **Angle(°)** | **Bond** | **Angle(°)** |
| N1–Co1–O3 | 86.4(4) | N1–Co1–O3W | 88.7(5) | N1–Co1–O2W | 97.0(5) |
| O1W–Co1–O4W | 88.6(6) | | | | |

**Table S4** Hydrogen bonds for compound **2**

| D–H···A | d(D–H) | d(H···A) | d(D···A) | <(DHA) |
|---|---|---|---|---|
| N3–H3B···O13#3 | 0.86 | 2.05 | 2.86(2) | 157.3 |
| N5–H5B···O39A | 0.86 | 2.73 | 3.12(3) | 109.2 |
| N7–H7A···O8W#4 | 0.86 | 1.51 | 2.06(5) | 118.2 |

Symmetry transformations used to generate equivalent atoms: #3 -x+2,-y+1,-z; #4 -x+2,-y,-z+1

**Table S5** Selected bond lengths (Å) and angles (°) for compound **3**

| Bond | Length(Å) | Bond | Length(Å) | Bond | Length(Å) |
|---|---|---|---|---|---|
| Cu1–N5 | 1.90(4) | Cu2–O4W | 2.58(7) | Cu5–O10W | 1.99(7) |
| Cu1–N1 | 1.91(4) | Cu3–O5W | 1.92(6) | Cu5–N17 | 2.02(4) |
| Cu1–O1W | 2.02(5) | Cu3–N13 | 1.94(4) | Cu5–O9W | 2.09(7) |
| Cu1–O47#1 | 2.04(3) | Cu3–O55 | 2.05(4) | Cu5–O74#6 | 2.11(3) |
| Cu1–O46 | 2.39(4) | Cu3–O6W | 2.07(6) | Cu5–O54 | 2.31(4) |
| Cu1–O2W | 2.63(10) | Cu3–O94#4 | 2.67(3) | Cu6–O12W | 1.93(6) |
| Cu2–N7#2 | 1.96(4) | Cu4–N15#5 | 1.95(5) | Cu6–N19#7 | 2.00(4) |
| Cu2–O3W | 1.96(5) | Cu4–O8W | 1.96(3) | Cu6–O11W | 2.03(5) |
| Cu2–N9 | 1.98(4) | Cu4–O71 | 2.03(3) | Cu6–O13W | 2.07(5) |
| Cu2–O68 | 2.12(4) | Cu4–O57#4 | 2.05(3) | Cu6–O65 | 2.27(3) |
| Cu2–O76#3 | 2.42(3) | Cu4–O7W | 2.19(4) | Cu6–O88#2 | 2.68(3) |
| **Bond** | **Angle(°)** | **Bond** | **Angle(°)** | **Bond** | **Angle(°)** |
| N5–Cu1–N1 | 173.4(18) | O76#3–Cu2–O4W | 169.4(17) | O10W–Cu5–N17 | 176(2) |
| N5–Cu1–O1W | 94.4(19) | O5W–Cu3–N13 | 96(2) | O10W–Cu5–O9W | 83(3) |
| N5–Cu1–O47#1 | 89.1(15) | O5W–Cu3–O55 | 155(2) | O74#6–Cu5–O54 | 142.2(14) |
| O46–Cu1–O2W | 159(2) | O6W–Cu3–O94#4 | 78.5(19) | O12W–Cu6–N19#7 | 94(2) |
| N7#2–Cu2–O3W | 93.4(19) | N15#5–Cu4–O8W | 175.0(18) | O12W–Cu6–O11W | 167(2) |
| N7#2–Cu2–N9 | 174.1(18) | N15#5–Cu4–O71 | 91.5(16) | O12W–Cu6–O13W | 87(2) |
| N7#2–Cu2–O68 | 92.0(15) | O57#4–Cu4–O7W | 102.1(13) | O65–Cu6–O88#2 | 164.2(12) |

Symmetry transformations used to generate equivalent atoms: #1 x-1,-y-1,z-1/2; #2 x,-y,z+1/2; #3 x-1,-y,z-1/2; #4 x,-y-1,z-1/2; #5 x+1,-y-1,z+1/2; #6 x,-y,z-1/2; #7 x+1,y,z+1

**Table S6** Hydrogen bonds for compound **3**

| D–H···A | d(D–H) | d(H···A) | d(D···A) | <(DHA) |
|---|---|---|---|---|
| N3–H3A···O107#8 | 0.86 | 2.28 | 3.08(7) | 156.7 |
| N12–H12A···O51#10 | 0.86 | 2.65 | 3.35(8) | 139.5 |
| N12–H12A···O20W#3 | 0.86 | 2.50 | 3.24(9) | 145.5 |
| N12–H12A···O27W#10 | 0.86 | 1.84 | 2.56(11) | 139.4 |

Symmetry transformations used to generate equivalent atoms: #3 x-1,-y,z-1/2; #8 x,-y-1,z+1/2; #10 x-1,y,z-1

**Table S7** Selected bond lengths (Å) and angles (°) for compound **4**

| Bond | Length(Å) | Bond | Length(Å) | Bond | Length(Å) |
|---|---|---|---|---|---|
| Zn1–N1 | 2.01(2) | Zn1–O1W | 2.155(13) | Zn2–O42#2 | 1.960(14) |
| Zn1–O2W | 2.051(17) | Zn1–O4W | 2.209(17) | Zn2–O5W | 2.17(3) |
| Zn1–O3W | 2.126(17) | Zn2–O18 | 1.896(14) | Zn2–O6W | 2.37(3) |
| Zn1–O28 | 2.133(13) | Zn2–N5 | 1.90(3) | | |
| **Bond** | **Angle(°)** | **Bond** | **Angle(°)** | **Bond** | **Angle(°)** |
| N1–Zn1–O2W | 177.4(9) | O1W–Zn1–O4W | 87.1(6) | O18–Zn2–O42#2 | 116.7(6) |
| N1–Zn1–O3W | 94.6(8) | O18–Zn2–N5 | 115.0(10) | O5W–Zn2–O6W | 172.2(11) |
| N1–Zn1–O28 | 95.0(7) | | | | |

Symmetry transformations used to generate equivalent atoms: #2 -x-1/2,y-1/2,-z+1/2

**Table S8** Hydrogen bonds for for compound **4**

| D–H···A | d(D–H) | d(H···A) | d(D···A) | <(DHA) |
|---|---|---|---|---|
| N4–H4A···O15#2 | 0.86 | 2.10 | 2.81(3) | 139.8 |
| N8–H8B···O29#3 | 0.86 | 2.44 | 3.27(2) | 161.1 |
| N8–H8B···O33#3 | 0.86 | 2.42 | 2.89(2) | 114.8 |
| N10–H10A···O50 | 0.86 | 2.42 | 3.87(3) | 113.5 |
| N10–H10A···O9W#4 | 0.86 | 2.54 | 3.17(4) | 131.3 |

Symmetry transformations used to generate equivalent atoms: #2 x+1/2, -y+13/2, z+1/2; #3 x, y-1, z; #4 -x-1/2, y+1/2, -z+1/2